Journal of
Polymer Materials

Tech Science Press

https://doi.org/10.32604/jpm.2026.080344

ARTICLE

Low-Velocity Impact Properties of Quad and Double-Double Composite Laminates

Muhammad Mudassar[1], Lei Cai[1], Qi Zhang[2] and Deng'an Cai[1,*]

[1]State Key Laboratory of Mechanics and Control for Aerospace Structures, Nanjing University of Aeronautics and Astronautics, Nanjing, China
[2]Shandong Province Key Laboratory for Electromagnetic Control and Multifunctional Integration Technology of Aerospace Electromagnetic Functional Structure, Research Institute for Special Structures of Aeronautical Composites, AVIC, Jinan, China

*Corresponding Author: Deng'an Cai. Email: cda@nuaa.edu.cn

Received: 07 February 2026; Accepted: 23 April 2026; Published: 30 June 2026

ABSTRACT: In this work, a comprehensive numerical study of the low-velocity impact (LVI) behavior of QUAD laminates vs. Double-Double (DD) stacking sequences has been performed. Finite element models were drawn, and analyses carried out in Abaqus/Explicit employing continuum shell elements (SC8R) for the plies, cohesive elements (COH3D8) for the delamination interfaces, and the built-in Hashin damage criterion for intralaminar failure. Two different impact energies (50 and 100 J) were applied using a hemispherical impactor mass of 6.25 kg, and the impact histories were investigated in force-time, displacement-time, and energy-absorption responses. The QUAD layup provided the stiffest response and highest peak contact forces, while it dissipated less energy, suggesting lower damage tolerance. Among the DD configurations, the variant designed for equal extensional stiffness (DI) had the lowest peak forces, the variant optimized with constraints on both extensional and bending stiffness (DIII) had the highest displacements and absorbable energies, and the variant designed for equal bending stiffness (DII) achieved intermediary results with values ranging appropriately when compared to QUAD. These results show that numerical simulation is able to reproduce the influence of stacking sequences on resistance and damage growth, which offers a more economical way to select laminate layups before experimental work. The simulations also indicate that the Double-Double design can result in distributed energy absorption due to increased delamination and matrix cracking, demonstrating its potential as a candidate design for impact-resistant structures.

KEYWORDS: QUAD laminates; double-double laminates; low-velocity impact; absorbed energy

1 Introduction

In the fiber-reinforced polymer (FRP) industry, QUAD 0°/±45°/90° laminates have established a state-of-the-art benchmark since the 1960s. They can be tailored with great versatility; changing the order of stacks or the fractions of each orientation allows engineers to tailor them to offer desired mechanical characteristics. But this flexibility can complicate the design stage. To further promote ease of layup and damage tolerance, however, common lay-up rules can be observed in relation to symmetry about the mid-plane, presence of at least 10% of a given ply angle for unexpected load bearing capabilities, keeping the number of plies having consecutive same-angled material properties to less than four to keep inter-laminar stress under control. However, despite these limits, the quantity of workable QUAD laminate arrangements is so great that optimization still represents a daunting task. Double-Double (DD) is a new construction scheme proposed by Tsai [1], which consists of 4-ply building blocks, such as $+\phi$, $-\phi$, $+\psi$, and $-\psi$ ply sequences. Instead of

coping with numerous ply layup orientations, the DD design laminate substantially reduces the complexity involved in design and fabrication by limiting such orientations to just four.

Several studies have been conducted since the development of DD laminates. Double-Double laminates are particularly promising in aerospace engineering as their building-block concept allows for easy optimization and manufacturing. This unique spatial freedom of double-double laminates (with ply drop-offs arranged at the outer surfaces of the batch) simplifies production even more [2]. An extensive study successfully identified the optimum design range for DD layups, enabling engineers to gain a better understanding of how composite laminates can be applied in practice across various industries [3]. For laminated composites, the ply stacking sequence affects the strength, stiffness, and buckling performance of the structure [4]. The classical laminate theory (CLT) and the mixed integer distributed ant colony optimization (MIDACO) method were used to determine the optimal stacking sequence, number of repeated blocks for the material system of composite panels, respectively, used in aircraft structures (wings, fuselage) [2]. Applying the new DD layup methodology, it becomes possible to reduce the number of plies required to achieve a certain specific strength and hence reduce the weight of this composite [5].

Composite structures such as those used in the aerospace and automotive industries are often impacted with low-velocity impacts (LVIs) from a variety of sources, including tool drop, hail, and bird strike. These quasi-static loading events give rise to complex damage states that include matrix cracking, fiber breakage, and interlaminar delamination [6,7]. Such damage modes usually occur under or below the impact surface, which are difficult to observe and can have a significant influence on residual strength and stiffness [8]. Composites are different from metals in that they do not plastically flow; instead, energy is dissipated primarily by micro-crack growth and delamination propagation. Knowledge of this process is important to enhance the crashworthiness and certification of composite aircraft panels [9]. As a result, numerical and experimental LVI studies have increasingly been emphasized as part of modern composite design approaches.

For single lap joints, the utilization of DD laminates with $\pm\Phi$ and $\pm\Psi$ ply-orientations provides possibilities for optimization owing to the fact that $0^\circ \leq \Phi < 90^\circ$ and $0^\circ \leq \Psi < 90^\circ$ are continuously optimized. Alves et al. [10] employed a finite element model to compare the performance of DD and QUAD laminates in a single lap joint, and found that the DD laminate performed better. Chang et al. [11] experimentally studied the LVI and compression-after-impact (CAI) performance of DD laminates. Through part using side-by-side within section testing against control legacy quad laminates (LQL), they reported for DD layups an up to 63% decrease in delaminated area and 4%–29% growth in residual compressive strength. The study proved that Double-Double laminates exhibited an improved impact resistance behavior as well as a retained structural integrity due to the manufacturing-friendly configuration and weight saving, which rendered them a viable candidate for aerospace and automotive applications requiring high damage tolerance. In addition to these findings, recent works have highlighted that DD laminates maintain comparable or superior performance even when compared to optimized hybrid or variable-stiffness designs [12]. For instance, Wang et al. [13] demonstrated that DD panels sustained higher post-impact compression strength due to distributed delamination fronts. Shang et al. [14] reported improved damage uniformity in tapered regions subjected to multi-axial loads. These results reinforce that the DD configuration provides an effective compromise between lightweight design, manufacturability, and impact resilience, particularly when supported by cohesive zone modeling and progressive damage simulations. Vermes et al. [15] performed the fatigue test in DD laminates with [±0/±25] and [±0/±50] building blocks and found similar fatigue behaviors to their equivalent QUAD, which indicated that DD laminates could be potential replacements. The study by Li et al. [16] is an example of how open-holes affect the failure and strength characteristics of DD laminates, in relation to conventional QUAD laminates, in proving one vs. the other (relative performance). It is revealed

that the size effect observed in QUAD laminates is not valid for DD laminates, thus showing higher strength with larger holes, indicating a potential of DD laminates for lightweight, efficient design applications.

Along with the DD laminates, other new composite architectures have been conceived that can help mitigate the shortcomings of traditional QUAD designs. Specifically, variable stiffness composites (VSCs), sometimes referred to as tow-steered or curvilinear fiber laminates, have been the subject of a significant amount of research focus. VSCs take advantage of the progress in automated fiber placement (AFP) technology to allow the continuous adjustment of fiber orientations along prescribed curved paths within a ply, eliminating the constraint of fixed angular orientations [17]. This spatial stiffness tailoring capacity produces great improvements in structural performance, which include enhanced buckling performance, post-buckling performance, slower onset of damage, and greater capacity to endure localized stress concentrations around cutouts. As an example, Lopes et al. [18] established that tow-steered panels had strength values that were 56% higher than straight fiber laminates when applied to uniaxial compressive loading. However, the capabilities of VSCs are often hindered by the complexities of manufacturing, such as the appearance of gaps and overlaps between tows, which may cause defects and local variations in thickness. Recent studies have been aimed at integrating manufacturing constraints into the optimization system in order to reduce such defects [1]. Even though VSCs are more tailorable, their production requires advanced AFP machinery and is difficult to control. By comparison, the DD concept offers a more practical tradeoff, with higher damage tolerance and design flexibility than QUAD laminates and still maintaining manufacturing simplicity due to its four-ply building-block design. The manufacturing vs. performance trade-off thus highlights the significance of exploring DD laminates in impact-resistant aerospace purposes.

In an investigation of the multiple impact responses and compression-after-impact (CAI) performance of composite laminates under different energy impacts, Hu et al. [19] examined the multiple LVI responses and compression-after-impact (CAI) performance of composite laminates. They found out that an initial impact can result in a given increase in impact resistance in cases where the impact energy is extremely small. The research provided useful information on cumulative damage behavior during repeated hits and attendant reduction of the residual strength. Zhang et al. [20] examined the LVI behavior of sandwich composites that used negative Poisson ratio lattice cores and showed that new architectural structures could affect the energy absorption and damage propagation processes. The findings of their paper highlighted the significance of central topology in impact energy distribution and the reduction of local damage. These works emphasize the important part played by numerical modeling in clarifying the development of impact damage and also give methodological backgrounds which guide the current exploration of Double-Double laminates under LVI.

To date, very few reports have been published on the LVI response of DD laminates. Dantas da Cunha et al. [21] studied the low velocity impact resistance of DD laminate for stacking sequence $[\pm 0/\pm 50]_{10}$ with that of QUAD laminate with equal stiffness and thickness $[0_3/90/\pm 45/0_2/\pm 45]_{2S}$. Compressive and CAI strengths were of similar magnitude; however, X-ray tomography revealed that the failure areas of both laminates differed in terms of delamination. DD laminates' delamination area was higher than that of QUAD laminates, because of less flexural stiffness. Millen et al. [22] quantitatively analyzed the LVI and CAI behavior of DD laminates. Results showed that DD laminates had higher CAI strength (up to 62%) and less delamination than conventional QUAD laminates with a weight savings of 25%–40%. They proposed DD laminates as a lightweight and damage-tolerant material that exhibited good performance compared with the traditional design method, holding corresponding potential for marine and aerospace structures. A study by Kappel et al. [23] analyzed QUAD and equivalent DD tapered laminates with similar in-plane stiffness [A] matrix to predict the performance of CAI under transition impacts. They found that DD laminates with ply drop-offs on their outer surfaces had lower CAI strengths when impacted in this critical region than those of the QUAD laminates. This demonstrates a compromise between the simpler DD design and

its structural integrity when subjected to damage. A recent article by Shabani et al. [12] evaluated the LVI and CAI behavior of DD and standard QUAD laminates using a three-dimensional (3D) finite element model. The results demonstrated that the impact damage tolerance and CAI properties of the DD laminates, designed to have equal in-plane stiffness [A] (or flexural stiffness [D]), were comparable with those for QUAD laminates, which can lead to manufacturing simplicity as well as more design flexibility. Key results revealed that the homogenization with minimum coupling phenomena could have been accomplished by optimized stacking sequence of DD laminates, such as $[\pm\phi/\pm\psi]_n$, at least even though they had slightly different performances according to the stiffness-matching criteria. The effort highlights DD laminates in this instance as an alternative to QUAD designs for aerospace applications where integrated design objectives require minimal structural efficiency with moderate difficulty in manufacturability. Prediction of LVI damage evolution has become efficient through the enhanced use of analytic finite element (FE) models, with Hashin and Puck criteria being an extensively used failure models [24]. Some new techniques, such as cohesive zone elements (CZEs), have been developed recently to predict the interlaminar delamination propagation, which can exhibit an improved correlation with the experimental observations [25]. Thorsson et al. [26] have experimentally validated these models on carbon/epoxy laminates. This indicates that explicit dynamic solvers, such as Abaqus/Explicit, can capture realistic contact and failing response at low-impulse duration rates. The application of both these frameworks and the use of laminate-based effects (ply drop-offs, gradient stiffness, and damage localization) that are at the heart of DD design optimization can be explored.

Although the LVI response of composite laminates has been extensively studied by many researchers, a common theme is to consider conventional quasi-isotropic or quadriaxial stacking sequences, or advanced user-defined material models, which require strict calibration. However, it can be argued that in certain applications, these are not feasible for engineering purposes. Considerably fewer attempts have been made in investigating DD laminate configuration with incorporated progressive damage tool only, despite their recent popularity for being an alternative design to enhance energy absorption and impact tolerance. In addition, detailed systematic numerical investigations on the performance of DD layups subjected to different impact energies are relatively scarce. To bridge this gap, the present work deals with multidirectional impact response analysis between a quadriaxial base and three DD configurations (DI, DII, and DIII) by numerical simulation with Abaqus/Explicit. Intralaminar damage is characterized using the implemented Hashin damage model, and delamination is modeled by a cohesive zone element between adjacent plies. The impact energies of 50 and 100 J with a hemispherical impactor are simulated, where the force-time histories, displacement-time histories, and absorbed energy are compared. The results offer an understanding of the effect of DD stacking sequence on impact resistance and the trade-off between stiffness-dominating response and energy-dissipation response. This study proves DD laminates are suitable for impact-reliable aSpplications, and it also shows the efficiency of numerical modeling as a cost-efficient methodology to be used in laminate design and analysis.

2 Materials and Methods

2.1 Conversion of QUAD Baseline to Double-Double Laminates

The (QUAD) baseline laminate was chosen as the reference state in this research, due to its well-balanced in-plane stiffness and also because it is widely used to study impact resistance. For a consistent comparison, three equivalent Double-Double (DD) laminates were used directly from the approach recently presented by Shabani et al. [12]. This conversion ensured that several design parameters, such as the total thickness, number of plies, balance, and symmetry, were maintained, allowing observed performance differences to be attributed solely to ply stacking architecture. As shown in Table 1, the first Double-Double (DI) laminate was made for an equal normalized stretch stiffness matrix [A*], for the second head (DII), an equal normalized

bending stiffness matrix [D*], and, finally, $|\Delta A^*| < 10\%$ and $|\Delta D^*| < 5\%$ imposed sagging stiffness (DIII). Such transformation of the QUAD baseline in DD laminates offers a uniform context to compare low velocity impact on these two layups with applied energy levels of 50 and 100 J. Equivalent laminates directly taken from [12] allow us to emphasize the influence of ply orientation strategy on load response, displacement, and damage while keeping constant both geometrical and material conditions.

Table 1: Lamination order taken from [12].

ID	Lamination Order	Attribute
QUAD	$[0/45/90/-45]_{4S}$	Baseline configuration
DI	$[67.5/-22.5/22.5/-67.5]_{8T}$	Equal [A*]
DII	$[64.5/-17/17/-64.5]_{8T}$	Equal [D*]
DIII	$[65.5/-18.5/18.5/-65.5]_{8T}$	Difference in [A*] < 10%, Difference in [D*] < 5%

2.2 Modeling and Pre-Processing

All computations were performed in Abaqus/Explicit solver (Dassault Systèmes, Vélizy-Villacoublay, France), a computer-based platform that is especially well adapted to LVI calculations due to its ability to handle extreme nonlinearities due to large deformations, cumulative damage, and complex contact interactions. The composite laminate was then modeled using the SC8R continuum shell element, which is an easy way of measuring through-thickness stresses without losing computational efficiency [26]. The ply itself was modeled by continuum shell elements that were oriented in the fiber direction in each ply, and each layer was a single ply. The chosen material system was the IM7/977-3 carbon-fiber-reinforced epoxy composite with constitutive parameters calculated based on Shabani et al. [12]. A finite-element model is shown in Fig. 1. The impactor was assumed to be a rigid hemisphere (25.4 mm diameter) with a mass of 6.25 kg, and the holder and clamping plates were also modeled as rigid bodies with R3D4 elements [27]. The hexahedron mesh was created using a local seed-by-size approach to control mesh density, as shown in Fig. 2. The unstructured hexahedrons mesh-maintained fiber aligned element orientation across the laminate thickness, so that stress fields at the ply level and interlaminar failure modes could be resolved precisely. Nodal seeding was limited to a minimum size of 0.5 mm × 0.5 mm in a refined 30 mm × 30 mm area under the impactor and to a maximum size of 2 mm × 2 mm along the plate edges, to form a dual-bias approach that enhances resolution in stress-concentration regions at a minimized computational cost.

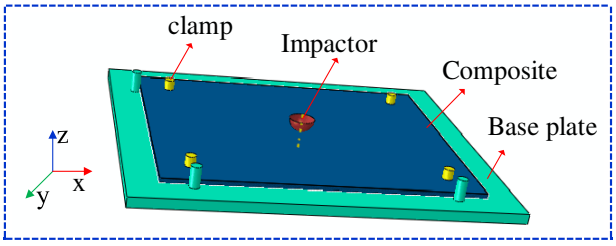

Figure 1: Finite element model.

The framework of Abaqus/Explicit was used to define contact interactions, such that the contact domain of "All with self" was used with the clamps and laminate, and laminate and support plate. Whereas surface to surface (Explicit) interaction was applied to impactor and laminate. Normal contact was modeled as "Hard" to discourage interpenetration, and the tangential response was modeled as a penalty friction formulation.

A friction coefficient of 0.8 was applied to the laminate-steel interface (clamps and support plate) to prevent slip, but a coefficient of 0.2 was used to represent the situation of low friction between the impactor and laminate. The clamps had a fully fixed boundary condition, and the impactor was constrained to translate in the thickness direction only.

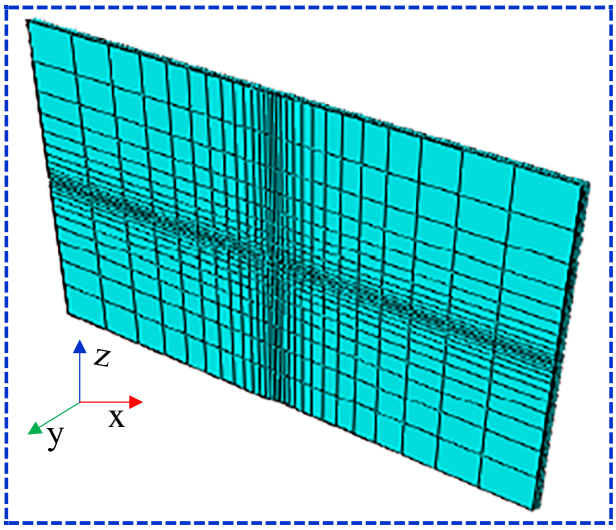

Figure 2: Meshing.

The built-in Hashin damage initiation criterion was used to model intralaminar damage [28]. The criterion was chosen based on its popularity and success in forecasting the onset of damage in fiber-reinforced polymer composites when subjected to LVI loads. It uses quadratic stress polynomials to distinguish between four different failure modes, which are fiber tension, fiber compression, matrix tension and matrix compression. This distinction is necessary to obtain the intralaminar damage evolution accurately in the LVI events, in which the matrix cracking is often observed before the fiber failure and delamination [29]. The ability of the criterion to model the mechanisms individually allows more physically realistic simulation of progressive damage than more simplistic interactive criteria as Hashin [28]. Recent research has demonstrated that the Hashin criterion, when used within a progressive damage model in Abaqus/Explicit, is able to provide exquisite fits with experimental data to both the force-time curves and damage morphology [30]. As an example, Thorsson et al. [26] compared continuum shell models, based on the Hashin, to compare experimental LVI data of carbon/epoxy laminates and obtained good predictive results in terms of peak forces, displacement, and damage extent. Our previous study of the numerical modeling of the evolution of composite damage has further supported the applicability of the Hashin criterion with LVI composite simulations [31]. Even though other criteria, like Puck, can offer a refined characterization of the matrix compression based on fracture-plane concepts [29], the Hashin criterion offers the best compromise in the accuracy and performance of the computational task in the current study of comparing several stacking sequences in a parametric way.

To simulate delamination, a sequence of cohesive elements (COH3D8) layers with a ply thickness of 0.005 mm was embedded between each layer, and a traction-separation law was used to model delamination initiation and propagation [32]. A quadratic nominal stress criterion controlled the initiation of damage, and the mixed-mode propagation was represented by the Benzeggagh-Kenane (BK) fracture criterion [33].

Numerical integration of the force-displacement response at the impactor reference node was used to calculate the absorbed energy. The integral of force in kilonewtons and displacement in millimeters, which

is the present model, returns energy in joules directly as in Eq. (1). To be more precise, the absorbed energy, E_{abs}, was determined by:

$$E_{abs} = \int F du \tag{1}$$

where F is the contact force (CFN3), and u is the impactor displacement (U3), which was determined between the starting point of contact and the final point of separation. This integral is therefore the energy lost in the damage mechanisms-matrix cracking, fiber breakage, delamination, and that lost in the friction during the impact event [34]. In simulations where the force acting is in the absence of gravity, this integral is directly proportional to the absorbed energy.

The impact energies of 50 and 100 J were chosen to outline two different damage regimes that are relevant to aerospace composite structures. The reduced energy (50 J) is consistent with the Barely Visible Impact Damage (BVID) at which point matrix cracking and delamination begin without any severe fiber failure, a critical design criterion to meet certification requirements [35]. The greater energy level (100 J) represents an extreme situation of impact where fiber fracturing is the leading cause, making it possible to test the performance of the fiber near the limit. The two discrete energy levels are sufficiently able to describe the transition between damage initiation and extensive failure, to provide useful information on the trade-off between stiffness and damage tolerance between QUAD and Double-Double laminates, without using unnecessary amounts of computational resources.

To determine the fidelity and mesh-independence of the numerical results, a systematic mesh convergence study was conducted, as shown in Fig. 3. The QUAD baseline laminate that was impacted at 50 J was selected as the experimental item because it is the most rigid configuration and has been studied in the current literature extensively. Four different mesh densities were examined, acquired through a series of gradual reductions of the size of the element within the impact zone: the coarse mesh (M1: 12,840 elements), the medium mesh (M2: 28,360 elements), the fine mesh (M3: 68,040 elements), and the very fine mesh (M4: 135,720 elements). Two main response variables were tracked: peak contact force (F_{max}) and maximum central displacement (δ_{max}), since these are the main indicators of the global impact response. Fig. 3 shows that both variables converged as the progressive refinement between M1 and M4 occurred. The fine mesh (M3, 68,040 elements) yielded values that were within 1.0% of the very fine mesh (M4, 135,720 elements) in terms of peak force (19.45 vs. 19.65 kN) and within 2.9% in terms of maximum displacement (1.75 vs. 1.80 mm when using the very fine mesh). Such differences are significantly lower than the traditional convergence threshold of 5% commonly used in engineering research. Based on this, all further simulations were henceforth carried out using the fine mesh structure (68,040 elements), which provides a reasonable compromise between the accuracy and the cost of simulation.

3 Results and Discussion

3.1 Force-Displacement Response

All trends in the following are based on our finite element method (FEM) simulations using Abaqus/Explicit. This configuration is commonly addressed to capture delamination-induced softening in LVI, as well as explaining the force-displacement (F-D) responses by means of the stiffness, damage initiation, and progressive energy dissipation. The F-D response accounts for the laminate indentation resistance against low-velocity impact, illustrating non-linearity with an initial quasi-linear region (elastic bending, local contact deformation), then involving stiffness degradation from intralaminar cracking and delamination. Peak force represents the load carrying capacity; the descending branch indicates a deteriorative process.

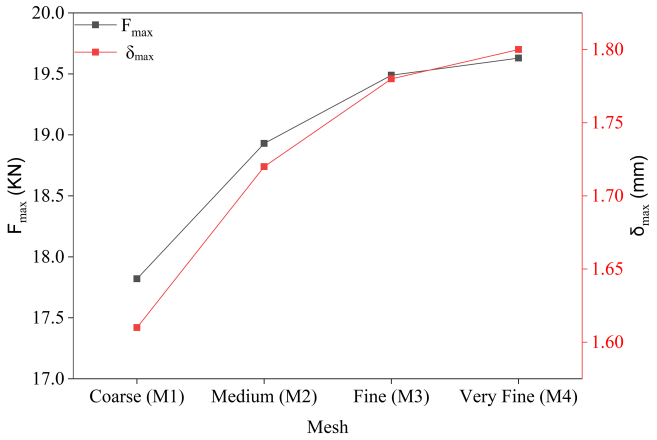

Figure 3: Mesh convergence study for QUAD laminate at 50 J impact.

Fig. 4 showed that at 50 J, the QUAD laminate had its peak force capabilities influenced by its stiffness properties, and the lowest displacement and energy absorbed until damage. Double-Double laminates (DI, DII, DIII) showed lower peaks of force, but higher displacement amplitudes, which suggested that Double–Double laminates were characterized by greater compliance. DIII showed the greatest displacement at maximum load with good deformation through delamination, and DI had the lowest peak force due to softer extensional stiffness. DII equated force-displacement response, approaching QUAD's baseline denoted by Q in what follows.

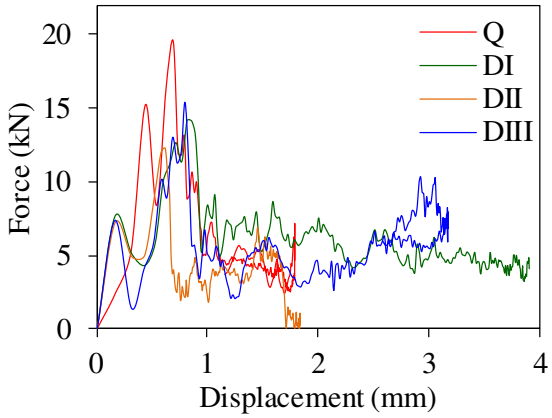

Figure 4: Force-displacement response at 50 J (overlay).

Fig. 5 showed the F-D results at 100 J having the enhanced dislocations and significant post-peak softening for all laminates. QUAD had the highest force but fast force drops, and peripheral low damage tolerance. Double-Double laminates had a smoother force drop and longer displacement, corresponding to gradual failure and better energy damping, with the DIII's deflection being about twice that of QUAD. These F-D responses illustrate a compromise between stiffness and damage tolerance, which is dominated by the stacking sequence optimization.

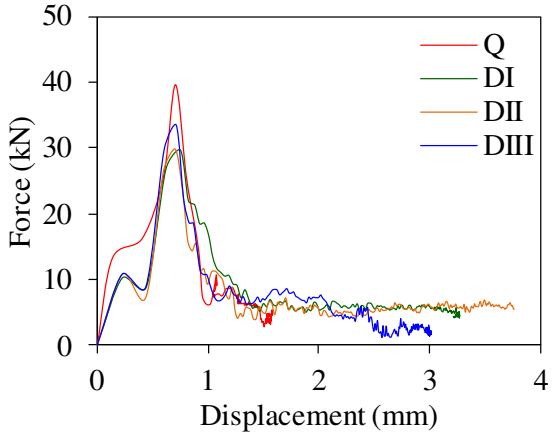

Figure 5: Force-displacement response at 100 J (overlay).

3.2 Force-Time Response

At both energies, the force-time (F-T) curves exhibit a sub-millisecond force ramp to the initial inflection impelled by the effective contact stiffness of the impactor-laminate system due to local indentation and global bending; after this initial period, overall ms-scale contact duration is characteristic of instrumented drop-weight LVI (ASTM D7136) and previous dynamics models. At 50 J (Fig. 6), the QUAD layup has a higher F_{max}, high-load dwell, and abrupt post-peak unloading, i.e., stiffness-dominated response, with little damage accommodation once interlaminar sliding initiates. By contrast, DIII (Double–Double) exhibits a smoother post-peak behavior and a wider high-load window, which agrees with a more gradual, diffuse-like fracture occurring here that moderates the unloading process, enhancing specific energy dissipation; DII retains symmetry (moderate peak dwell), whereas DI is the softest one. This peak sharpness vs. dwell pattern is a well-known LVI signature, which connects architectural stiffness with the force-decay rate following propagation of damage.

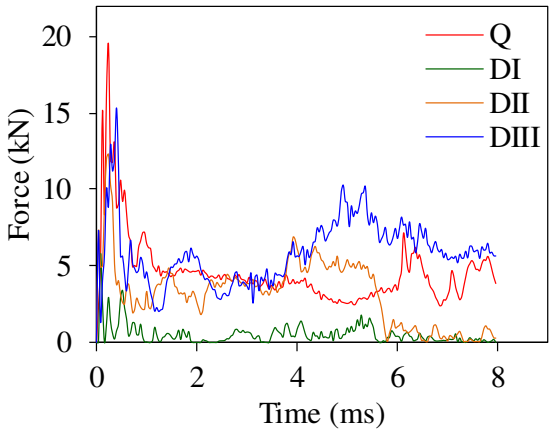

Figure 6: Force-time response at 50 J (overlay).

At 100 J of impact energy (Fig. 7), increased energy maintains the early high rigid force development but higher peak displacement and post-peak softening of all stacks. Again, QUAD shows the highest F_{max} but exhibits a steeper force drop (track rapid load relaxation), suggesting less resistance to damage at higher energy. DD configurations (especially DIII) exhibit a more rounded peak and longer high-load dwells,

indicating stable multi-site delamination and high dissipated energy before rebound, while DII still trades on slight peak reduction for extended load transfer. In summary, the F-T responses at 50 and 100 J unveil the predictable stiffness-toughness trade-off: stiffer QUAD exhibited sharper peak and faster decay; more compliant DD showed wider dwell and progressive unloading.

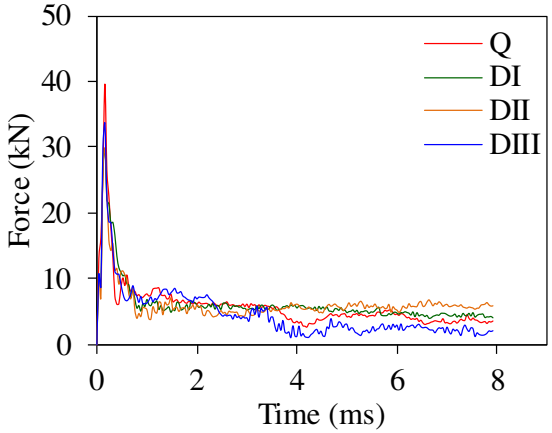

Figure 7: Force-time response at 100 J (overlay).

3.3 Displacement-Time Response

The traces of displacement-time (D-T) at 50 J (Fig. 8) illustrate an important performance off. QUAD laminate exhibits higher stiffness and limited plastic deformation by recording the least peak displacement. In contrast, the DI laminate permits higher peak displacement and a longer post-peak dwell time, stating simply that more strain energy is stored and active mode-I delamination initiates at an earlier location. DII laminate is balanced, with maximum displacement and recovery occurring between DI and DIII laminates; DIII laminate reaches the maximum displacement and has the slowest recovery, indicating successive, multiple-site delamination leading to increasingly more energy dissipation before full bounce back.

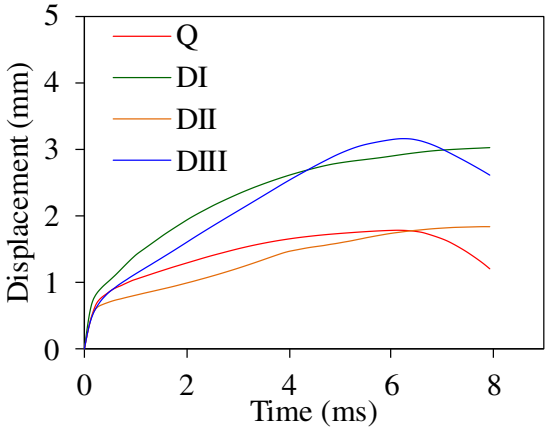

Figure 8: Displacement-Time response at 50 J (overlay).

For 100 J (Fig. 9), all layup strategies record greater peak displacement (D_{max}) and longer recovery, but relative hierarchy is independent of applied energy; however, QUAD assumes the least δ_{max} and fastest rebound, DI and DII follow in both peak and dwell (with DII reconfirmed to hold a balanced face-diagonal),

and now, once more, DIII gives rise to the greatest D_{max} together with longest recoil. In general, D-T histories indicate that the greater the impact energy, deflection, and rebound are increased, while the stacking sequence determines how strain energy is stored and released, with QUAD favoring small deflections with rapid snap-back and Double–Double designs, particularly DIII, favoring larger, slowly recovering displacements akin to higher damage tolerance.

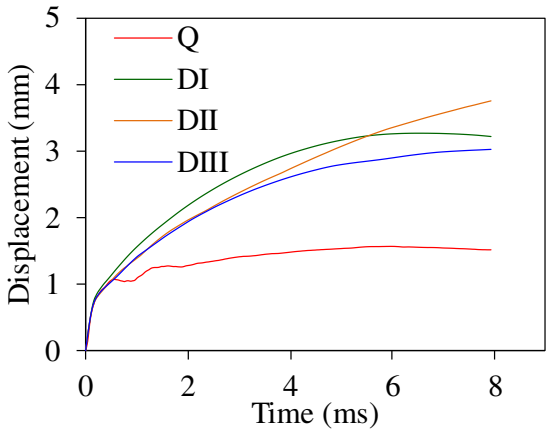

Figure 9: Displacement-time response at 100 J (overlay).

To demonstrate the spatial distribution of deformation and damage, contour plots of the maximum point of displacement at an impact of 100 J are shown in Fig. 10. Fig. 10a,c shows the out-of-plane displacement contours which define different patterns of deformation of the two laminates. The QUAD laminate (Fig. 10a) has a very localized displacement field with the highest displacement at the bottom of the impactor which is 2.63 mm. Conversely, the DIII laminate (Fig. 10c) exhibits a more widespread, spread displacement field up to 3.94 mm, which is evidence of increased compliance and the involvement of a greater volume of material upon impact. This is a large expansion deformation pattern which is directly relatable to the increased energy absorption of DIII (26.22 J) compared to QUAD (22.26 J) at the impact level of 100 J.

Contours Fig. 10b,d shows the damage-initiation criterion (DMICRTMAXVAL) and illustrate the distribution and magnitude of the damage. In the case of the QUAD laminate (Fig. 10b) those areas where DMICRTMAXVAL is large (indicated by red color) are significantly concentrated under the impactor, indicating localized damage. On the contrary, the DIII laminate (Fig. 10d) has a more scattered pattern of damage, as the damage is spread in a wider area. This morphology of distributed damage is the reason why DIII has a superior energy absorption, because energy is wasted over a greater area as opposed to localized failure. The wider spread of damage in DIII also indicates a better potential to residual strengths as the region of damaged may not act as a critical stress concentrator when subjected to further compressive force. All of these visual observations support the quantitative results and indicate that the Double-Double architecture has a higher damage tolerance.

3.4 Impact Key Performance Indicators

Quantification of different damages is figured out based on the analysis of 50 J impact key performance indicators (Table 2). With low maximum displacement and fast rebound, the QUAD laminate is characterized by a high stiffness to resist larger damage accommodation. Whereas DI possesses a priority for compliant energy storage and premature delamination growth (with larger maximum displacement and longer dwell), DII presents an intermediate behavior, while DIII claims the best damage tolerance (with the

highest maximum displacement to achieve more effective progressive failure). The results substantiate two key principles. First, DIII laminate is uniquely efficient in terms of damping, having maximum hysteresis energy and delayed rebound to promote cumulative damage propagation and increase damping. Second, the uniform duration of contact ($t_c \approx 7–8$ ms) among all configurations indicates that the time scale for the impact event is not determined by the given stacking sequence; instead, it reflects the energy brought into the target by impact.

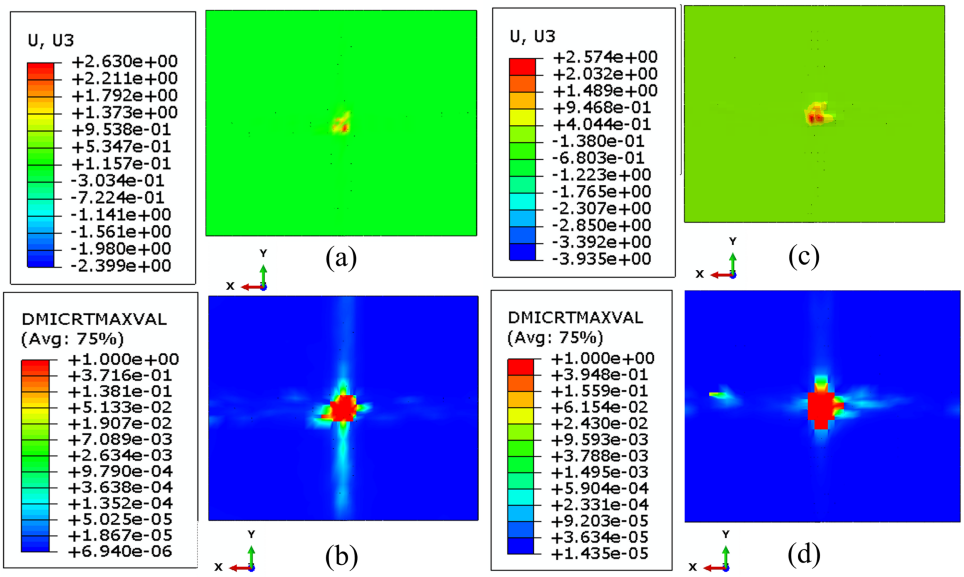

Figure 10: Contour plots at the moment of maximum displacement for 100 J impact: (**a**) out-of-plane displacement (U3, mm) for QUAD laminate; (**b**) combined damage-initiation criterion for QUAD laminate; (**c**) out-of-plane displacement (U3, mm) for DIII laminate; (**d**) combined damage-initiation criterion for DIII laminate.

Table 2: Impact key performance indicators.

Energy (J)	Layup	Peak Force (kN)	Max Displacement (mm)	Impact Duration (ms)
50	Q	19.49	1.78	7.96
50	DI	5.8	0.24	7.08
50	DII	12.31	1.83	7.84
50	DIII	15.4	3.16	7.96
100	Q	39.72	1.57	7.96
100	DI	29.8	3.27	7.96
100	DII	29.82	3.76	7.96
100	DIII	33.54	3.01	7.96

At the higher energy level of 100 J, the same failure modes drive the improved behavior. The QUAD laminate is the stiffest, which has the most deflection but the fastest recovery. The maximum displacement and the dwell time of the DD laminates, set DI and DII, were also at the same level, while DIII again resulted in the largest maximum displacements and slowest rebound by consuming higher energy progressively. Contact time is also the same, still 7–8 ms at the impact energy of 100 J, which indicates that the event timescale is governed by loading energy, whereas the design layup determines its dissipation strategy. This distinction

reveals that elastic response and prompt recovery are appropriate for the QUAD laminate, whereas the stiffness of the DD design, in particular DIII, is sacrificed to achieve better damage tolerance by prolongation of energy dissipation.

The absorbed energy and corresponding efficiency values, as displayed in Table 3 and plotted in Fig. 11, reveal important details on the energy dissipation characteristic of the laminates. At 50 J, the Double-Double variants showed greater absorption with DI absorbing 23.9 J (48% efficiency) and DIII absorbing 17.25 J (34%), while QUAD absorbed just 12.01 J (24%).

Table 3: Absorbed energy and efficiency.

Energy (J)	Layup	Absorbed Energy (J)	Absorption Efficiency (E_{abs}/E_0)
100	DI	30.22	0.3
100	DII	29.82	0.3
100	DIII	26.22	0.26
100	Q	22.26	0.22
50	DI	23.9	0.48
50	DII	8.34	0.17
50	DIII	17.25	0.34
50	Q	12.01	0.24

The results show that DD laminates dissipate impact energy effectively by damage modes of matrix cracking and delamination. At 100 J, this trend continued with 30 J being absorbed by DI and DII shields (i.e., 30% efficiency) while QUAD only absorbed 22.26 J (22%). The results offer evidence of higher displacement potential for Double-Double laminates, which leads to highly increased energy absorption and, therefore, are suitable for impact tolerance and crashworthiness.

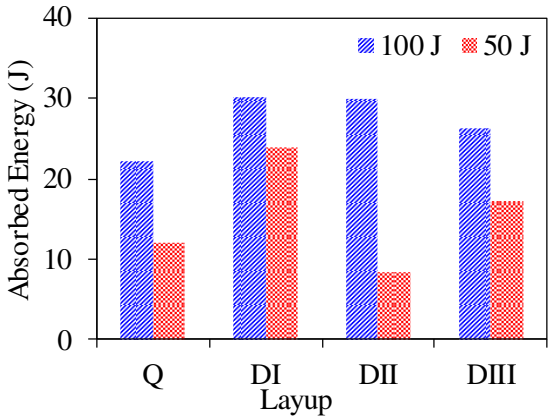

Figure 11: A comparison of absorbed energy for 50 and 100 J impact energies.

3.5 Implications for Residual Strength and Aerospace Design

In spite of the fact that no compression after impact (CAI) testing was part of this numerical study, the damage mechanisms implied are valuable indicators of the predicted residual compressive capacity of composite laminates. In composite laminates, residual compressive strength is significantly controlled by the level as well as the geometrical pattern of what is caused by impact, especially delamination. Localized

damage produces stress concentrations that enable buckling under compression but a widely spread pattern of damage spreads the load applied over a greater area and reduces values of peak stress concentrations. The DIII laminate also showed a more diffused pattern of matrix cracking and delamination (Fig. 10), which implies that it would perform better at CAI than QUAD laminate, which showed localized damage under the impactor. This finding is in agreement with experimental studies that indicate up to 62% greater CAI strength of DD laminates compared to an equivalent setup of QUAD. In terms of actual structure performance, the fact that the DD laminates exhibit greater energy absorption (34% at 50 J compared to 24% at 50 J in QUAD) means that the DD laminates are better crashworthy in terms of the aerospace industry where impact events such as runaway debris or bird strikes are design critical. The increased compliance of DD laminates also implies increased ability to absorb impact without catastrophic failure though at a cost of reduced peak load capacity. In the case of stiff components (such as wing skins), QUAD laminates are still considered superior when the greatest load-bearing capacity is desired as opposed to energy absorption features.

Design guidelines: (a) QUAD laminates are applicable in rigidly demanding impact-sensitive applications; (b) DIII laminates are used in structures being damage-sensitive and those demand the use of large amounts of energy; (c) DII laminates are balanced general-purpose aerospace components; (d) DI laminates are used in energy-absorbing substructures where progressive failure is required.

4 Conclusion

The FE simulations carried out in the present work provided a new understanding of the low-velocity impact response of Double-Double laminates compared with a quadriaxial reference. The QUAD layup demonstrated the highest peak force reactions in both 50 and 100 J impacts, indicating stiff but low damage-tolerant behavior. In contrast, in Double-Double sequences, the stresses were relocated by their characteristic $\pm\phi/\pm\psi$ orientation pattern, which enabled higher-energy dissipation by intralaminar cracking and interlaminar delamination. Regarding partial failure, DI presented the lowest force (indicating a softer impact response), DIII had the largest displacement and absorption energy ratio (being therefore most damage-tolerant), and DII was an intermediate solution characterized by moderate stiffness combined with increased energy dissipation.

Present work shows that modelling is possible with Abaqus/Explicit using Hashin's intralaminar damage model and cohesive zone elements to accurately predict laminate impact performance without recourse to expensive testing. The reported results confirm the versatility of Double–Double tailored-impact response through ply orientation manipulation. In other words, Double-Double laminates are appropriate for applications involving energy absorption and damage tolerance over maximum load capabilities, and provides a basis for which advanced composite layups may be further optimized.

The existing model assumes perfect bonding and does not consider manufacturing defects such as voids and fiber waviness, or partial final thermal stresses that can affect damage initiation. Despite its computational efficiency, the Hashin criterion fails to resolve the elusive fracture plane angle in matrix compression compared with Puck's criterion. Effects that are dependent on strain-rate on material properties are also not present in the current formulation. These limitations should be overcome by future studies by experimentally validating DD configurations and by investigating reduced-order modelling methods.

Acknowledgement: None.

Funding Statement: This work was partially supported by the National Natural Science Foundation of China (Grant No. 52005256), the grant from Shandong Province Key Laboratory for Electromagnetic Control and Multifunctional Integration Technology of Aerospace Electromagnetic Functional Structure, Research Institute for Special

Structures of Aeronautical Composites, AVIC and the Priority Academic Program Development of Jiangsu Higher Education Institutions.

Author Contributions: The authors confirm contribution to the paper as follows: Conceptualization, Deng'an Cai; methodology, Muhammad Mudassar and Lei Cai; software, Muhammad Mudassar; validation, Deng'an Cai and Qi Zhang; formal analysis, Lei Cai; investigation, Muhammad Mudassar and Lei Cai; resources, Deng'an Cai; data curation, Muhammad Mudassar and Lei Cai; writing—original draft preparation, Muhammad Mudassar and Lei Cai; writing—review and editing, Qi Zhang and Deng'an Cai; visualization, Lei Cai and Qi Zhang; supervision, Deng'an Cai; project administration, Deng'an Cai; funding acquisition, Deng'an Cai. All authors reviewed and approved the final version of the manuscript.

Availability of Data and Materials: The authors confirm that the data supporting the findings of this study are available within the article.

Ethics Approval: Not applicable.

Conflicts of Interest: The authors declare no conflicts of interest.

References

1. Tsai SW. Double–double: new family of composite laminates. AIAA J. 2021;59(11):4293–305. doi:10.2514/1.j060659.
2. Kappel E. Double–double laminates for aerospace applications—finding best laminates for given load sets. Compos Part C Open Access. 2022;8:100244. doi:10.1016/j.jcomc.2022.100244.
3. Zhao K, Kennedy D, Miravete A, Tsai SW, Featherston CA, Liu X. Defining the design space for double–double laminates by considering homogenization criterion. AIAA J. 2023;61(7):3190–203. doi:10.2514/1.j062639.
4. Shonkwiler S, Li X, Fenrich R, McMains S. Deep reinforcement learning for stacking sequence optimization of composite laminates. Manuf Lett. 2023;35:1203–13. doi:10.1016/j.mfglet.2023.08.133.
5. Vermes B, Tsai SW, Massard T, Springer GS, Czigany T. Design of laminates by a novel "double–double" layup. Thin Walled Struct. 2021;165:107954. doi:10.1016/j.tws.2021.107954.
6. Qiu J. Research and analysis on low-velocity impact of composite materials. Sci Eng Compos Mater. 2023;30(1):20220209. doi:10.1515/secm-2022-0209.
7. Bogenfeld R, Kreikemeier J, Wille T. Review and benchmark study on the analysis of low-velocity impact on composite laminates. Eng Fail Anal. 2018;86:72–99. doi:10.1016/j.engfailanal.2017.12.019.
8. Ferreira LM, Coelho CACP, Reis PNB. Effect of cohesive properties on low-velocity impact simulations of woven composite shells. Appl Sci. 2023;13(12):6948. doi:10.3390/app13126948.
9. Anuse VS, Shankar K, Velmurugan R, Ha SK. Compression-after-impact analysis of carbon fiber reinforced composite laminate with different ply orientation sequences. Int J Impact Eng. 2022;167:104277. doi:10.1016/j.ijimpeng.2022.104277.
10. Alves GC, Vignoli LL, Neto RMC. Damage onset in CFRP single lap joint for DD and QUAD laminates. J Mech Sci Technol. 2024;38(1):157–62. doi:10.1007/s12206-023-1213-z.
11. Chang Z, Gao Y, Chen J, Zhao J, He L, Zhao Y, et al. Experimental investigation of the low velocity impact behavior and residual compressive strength of a novel double–double layup composite laminates. Polym Compos. 2025;46(11):9973–86. doi:10.1002/pc.29598.
12. Shabani P, Li L, Laliberte J. Low-velocity impact (LVI) and compression after impact (CAI) of double-double composite laminates. Compos Struct. 2025;351:118615. doi:10.1016/j.compstruct.2024.118615.
13. Wang X, Zhang W, Lu S, Zhang L, Ma C, Zhao W, et al. Numerical study on the secondary impact response of double-double composite laminates. Appl Compos Mater. 2025;33(1):15. doi:10.1007/s10443-025-10400-x.
14. Shang Y, Ma X, Feng C, Ding Y, Ma K. Study of low-velocity impact damage in composite laminates based on crack energy. Fibers. 2025;13(9):115. doi:10.3390/fib13090115.

15. Vermes B, Tsai SW, Riccio A, Di Caprio F, Roy S. Application of the Tsai's modulus and double-double concepts to the definition of a new affordable design approach for composite laminates. Compos Struct. 2021;259(11):113246. doi:10.1016/j.compstruct.2020.113246.
16. Li X, Lv X, Jiang T, Zhao Q, Rao W, Li Y, et al. Size effect and damage mechanism of Double–Double open-hole composite laminates. Compos Sci Technol. 2025;266(1):111158. doi:10.1016/j.compscitech.2025.111158.
17. Pagani A, Racionero Sánchez-Majano A, Zamani D, Petrolo M, Carrera E. Fundamental frequency layer-wise optimization of tow-steered composites considering gaps and overlaps. Aerotec Missili Spazio. 2025;104(2):135–51. doi:10.1007/s42496-024-00212-w.
18. Lopes CS, Camanho PP, Gürdal Z, Tatting BF. Progressive failure analysis of tow-placed, variable-stiffness composite panels. Int J Solids Struct. 2007;44(25–26):8493–516. doi:10.1016/j.ijsolstr.2007.06.029.
19. Hu P, Jian YA, Hu C, Zhang N, Wang X, Cai DA, et al. On multiple low-velocity impact response and compression after impact of composite laminates. Mech Adv Mater Struct. 2025;32(6):1043–57. doi:10.1080/15376494.2024.2358515.
20. Zhang Y, Cai DA, Peng J, Qian Y, Wang X, Miao L. On low-velocity impact behavior of sandwich composites with negative Poisson's ratio lattice cores. Compos Struct. 2022;299(1):116078. doi:10.1016/j.compstruct.2022.116078.
21. Dantas da Cunha R, Targino TG, Cardoso C, Paiva da Costa Ferreira E, Freire RCSJr, Daniel Diniz Melo J. Low velocity impact response of non-traditional double-double laminates. J Compos Mater. 2023;57(10):1807–17. doi:10.1177/00219983231163513.
22. Millen SL, Aravand MA, Ullah Z, Falzon BG. Studies on the impact and compression-after-impact response of 'double-double' carbon-fibre reinforced composite laminates. In: double-double: simplifying the design and manufacture of composite laminates. Stanford, CA, USA: Stanford University; 2023. p. 161–80.
23. Kappel E, Boose Y, Mißbach M. A CAI study on transition zones of conventional and double-double laminates. Compos Part C Open Access. 2024;14(3):100450. doi:10.1016/j.jcomc.2024.100450.
24. Patil S, Mallikarjuna Reddy D. Study of oblique low velocity impact on composite plate. Mater Today Proc. 2021;46(5):9433–7. doi:10.1016/j.matpr.2020.03.125.
25. Turon A, Costa J, Camanho PP, Dávila CG. Simulation of delamination in composites under high-cycle fatigue. Compos Part A Appl Sci Manuf. 2007;38(11):2270–82. doi:10.1016/j.compositesa.2006.11.009.
26. Thorsson SI, Waas AM, Rassaian M. Low-velocity impact predictions of composite laminates using a continuum shell based modeling approach Part b: BVID impact and compression after impact. Int J Solids Struct. 2018;155(4):201–12. doi:10.1016/j.ijsolstr.2018.07.018.
27. Shi Y, Swait T, Soutis C. Modelling damage evolution in composite laminates subjected to low velocity impact. Compos Struct. 2012;94(9):2902–13. doi:10.1016/j.compstruct.2012.03.039.
28. Hashin Z. Fatigue failure criteria for unidirectional fiber composites. J Appl Mech. 1981;48(4):846–52. doi:10.1115/1.3157744.
29. Li F, Jin S, Li W, Luo Z. Assessment of damage prediction models for composite laminates under single and repeated low-velocity impacts. Aerosp Sci Technol. 2024;155:109633. doi:10.1016/j.ast.2024.109633.
30. Zhang Y, Van Paepegem W, De Corte W. An enhanced progressive damage model for laminated fiber-reinforced composites using the 3D hashin failure criterion: a multi-level analysis and validation. Materials. 2024;17(21):5176. doi:10.3390/ma17215176.
31. Deng J, Zhou G, Bordas SPA, Xiang C, Cai D. Numerical evaluation of buckling behaviour induced by compression on patch-repaired composites. Compos Struct. 2017;168(13):582–96. doi:10.1016/j.compstruct.2016.12.071.
32. Turon A, Camanho PP, Costa J, Dávila CG. A damage model for the simulation of delamination in advanced composites under variable-mode loading. Mech Mater. 2006;38(11):1072–89. doi:10.1016/j.mechmat.2005.10.003.
33. Benzeggagh ML, Kenane M. Measurement of mixed-mode delamination fracture toughness of unidirectional glass/epoxy composites with mixed-mode bending apparatus. Compos Sci Technol. 1996;56(4):439–49. doi:10.1016/0266-3538(96)00005-X.

34. Belingardi G, Vadori R. Low velocity impact tests of laminate glass-fiber-epoxy matrix composite material plates. Int J Impact Eng. 2002;27(2):213–29. doi:10.1016/S0734-743X(01)00040-9.
35. Chow ZP, Gliszczynski A. Finite element analyses of thin GFRP panels under low-velocity impact: damage assessment from Barely Visible Impact Damage (BVID) to perforation. Int J Impact Eng. 2025;206(12):105441. doi:10.1016/j.ijimpeng.2025.105441.